Article

Hierarchical Model Predictive Control for Hydraulic Hybrid Powertrain of a Construction Vehicle

Zhong Wang and **Xiaohong Jiao** *

School of Electrical Engineering, Yanshan University, Qinhuangdao 066004, China; wangzhong@stumail.ysu.edu.cn
* Correspondence: jiaoxh@ysu.edu.cn

check for updates

Abstract: Hybrid hydraulic technology has the advantages of high-power density and low price and shows good adaptability in construction machinery. A complex hybrid powertrain architecture requires optimization and management of power demand distribution and an accurate response to desired power distribution of the power source subsystems in order to achieve target performances in terms of fuel consumption, drivability, component lifetime, and exhaust emissions. For hybrid hydraulic vehicles (HHVs) that are used in construction machinery, the challenge is to design an appropriate control scheme to actually achieve fuel economy improvement taking into consideration the relatively low energy density of the hydraulic accumulator and frequent load changes, the randomness of the driving conditions, and the uncertainty of the engine dynamics. To improve fuel economy and adaptability of various driving conditions to online energy management and to enhance the response performance of an engine to a desired torque, a hierarchical model predictive control (MPC) scheme is presented in this paper using the example of a spray-painting construction vehicle. The upper layer is a stochastic MPC (SMPC) based energy management control strategy (EMS) and the lower layer is an MPC-based tracking controller with disturbance estimator of the diesel engine. In the SMPC-EMS of the upper-layer management, a Markov model is built using driving condition data of the actual construction vehicle to predict future torque demands over a finite receding horizon to deal with the randomness of the driving conditions. A multistage stochastic optimization problem is formulated, and a scenario-based enumeration approach is used to solve the stochastic optimization problem for online implementation. In the lower-layer tracking controller, a disturbance estimator is designed to handle the uncertainty of the engine, and the MPC is introduced to ensure the tracking performance of the output torque of the engine for the distributed torque from the upper-layer SMPC-EMS, and therefore really achieve high efficiency of the diesel engine. The proposed strategy is evaluated using both simulation MATLAB/Simulink and the experimental test platform through a comparison with several existing strategies in two real driving conditions. The results demonstrate that the proposed strategy (SMPC+MPC) improves miles per gallon an average by 7.3% and 5.9% as compared with the control strategy (RB+PID) consisting of a rule-based (RB) management strategy and proportional-integral-derivative (PID) controller of the engine in simulation and experiment, respectively.

Keywords: hybrid hydraulic vehicle (HHV); energy management strategy (EMS); setpoint tracking; model predictive control (MPC); Markov model; stochastic optimization

1. Introduction

The development of clear and efficient city transportation is of significant importance to the solutions for energy shortages and environmental issues. A vehicle with a hybrid powertrain is of great interest as a typical representative of environmentally friendly and efficient fuel usage [1]. Usually,

hybrid electric power is the standard approach to improve powertrains for passenger cars, whereas hybrid hydraulic power is an interesting alternative for heavy vehicles, such as city buses, commercial trucks, and construction vehicles. This is due to the superior ability of the hydraulic accumulator to accept high rates and high frequencies of charging and discharging, and therefore cope with operating conditions that involve frequent load changes [2,3]. Accordingly, hybrid hydraulic vehicles (HHVs) are usually characterized by lower travel speed, more obvious periodicity, higher amplitude and load change rate, as well as frequent start-stop operations [4,5].

For hybrid power systems, the controlling distribution of the power demand between the engine and the electrical or hydraulic motors, namely the energy management control strategy (EMS), is crucial to the reduction of fuel consumption while satisfying performance constraints. Compared to hybrid electric vehicles (HEVs), to date, there have been relatively few related researches on HHVs. Although the proven techniques for controlling HEVs are used as reference, there is still a need to develop control strategies tailored specifically to HHVs. In particular, the relatively low energy density of a hydraulic accumulator requires a carefully designed control strategy in order for the fuel economy potential to be fully realized.

In practice, the EMS for HHVs is usually designed as a rule-based (RB) control strategy because it is simple and has real-time implementable structure [6–10]. However, since its control performance depends heavily on rule-switching thresholds defined by the engineering experience, it actually cannot always provide good results during various driving conditions. Therefore, in order to achieve the best control performance possible during a driving cycle, an optimization-based control strategy has become a popular research topic for HHVs, as well as for HEVs. If the driving cycle is completely known, dynamic programming (DP) [11–13] should be the most popular optimization-based EMS. However, due to the uncertain real driving cycles, the EMS designed offline based on DP is not feasible in practice, although it is globally optimal in theory. Consequently, stochastic DP (SDP) [14] is a natural alternative to DP, which utilizes the probability distribution extracted from multiple historical driving cycles to deal with the uncertain driving cycles in practice. From the aspect of a real-time implementable EMS, the equivalent consumption minimization strategy (ECMS) [15] is a popular instantaneous optimization-based method. However, to be close to global optimization, it is a challenge to determine an appropriate adaptive equivalent factor for ECMS. Fortunately, EMS that uses a model predictive control (MPC) framework achieves both near-global optimization and real-time implementation provided the prediction model in the MPC is well processed and the real-time performance of the solution algorithm to the optimal control in the finite receding horizon is guaranteed. In this regard, a MPC-based control strategy is highly adoptable in the design of EMS for HHVs, and therefore more efforts have been directed at the model's prediction accuracy and a real-time optimal solution. More specifically, an MPC-based EMS is designed in [16] for a parallel HHV used in a passenger vehicle, in which the optimization objective is only a convex quadratic function that can be solved quickly to avoid the requirement of intense online computations. To improve the prediction performance, a type of predictive energy management approach with a learning drive cycle based on previous vehicle operations on the same route is presented in [17] for parallel hydraulic hybrid powertrain heavy vehicles used in garbage trucks or city buses. Moreover, in [18], the learned driving profiles for the prediction are associated with a particular vehicle's location. An MPC energy management method is studied in [19] for a series HHV based on the prediction of engine power by means of decrement of velocity tracking error. Additionally, an MPC-based EMS is presented in [20] for a type of parallel HHV based on the prediction model using the simplified powertrain dynamics to facilitate rapid online solutions to the optimization problem. However, it should be noted that, in practice, the uncertain driving cycles inevitably affect the accuracy of the prediction information and further affect the control performance of the MPC-based EMS. Therefore, stochastic model predictive control (SMPC) is a promising approach in an EMS, such as, in [21], where the velocity demand from the driver is expressed as a random Markov process and a SMPC strategy is developed for power management tailored for the series HHV.

In a vehicle with a hybrid powertrain that involves an engine, the upper-layer EMS controls the power allocation between the engine and the additional power source which is undoubtedly crucial to reduce fuel consumption and exhaust emission; however, the lower-layer closed-loop control of the driving power source itself, especially the engine, is even more important to realize the effect of the EMS. To this end, several researchers have focused on the lower-layer control design of an engine and pump/motor to achieve the power split for HHVs. For example, in [22], the engine on/off control strategy based on compensation of the used accumulator power is investigated and the effect of control parameters on the performance and efficiency of the hybrid power train is analyzed for improvement of fuel economy. The design and evaluation of the linear MPC method is presented in [23] applied to the tracking problem in a hydraulic hybrid powertrain system. A strategy that combined steady-state feedforward control with an MPC-based dynamic control is designed in [24] to calculate the control input sequence of engine torque and hydraulic variable pump displacement for a heavy commercial vehicle. However, it is worth mentioning that the influence of uncertainties of the system structure and parameters, as well as external disturbance, is not ignored on the transient and static performance of the closed-loop control of the subsystems of the HHVs.

Motivated by the analysis above, in this study, we focus on a hierarchical control including upper-layer EMS and lower-layer engine closed-loop control to implement optimal engine control with high efficiency and low fuel consumption for a hydraulic hybrid powertrain used in an example of a spray-painting construction vehicle. The structural feature of the HHV uses a hydraulic bridge and one accumulator to achieve two-way energy collection, which is different from the usual structure of most HHVs that use two accumulators with high and low pressures. Considering the uncertain acceleration and deceleration driving cycles of the construction vehicle studied, the uncertain nonlinear characteristics of engine and external disturbance, as well as the actuator constraints, a hierarchical MPC strategy is designed to achieve reasonable distribution of engine power and obtain better performance of setpoint tracking of engine torque. The main highlights of the proposed control strategy include three aspects. First, the uncertain driving cycle derived from the randomness of drivers' driving patterns of construction vehicles and considered and a SMPC-EMS is proposed, to predict the acceleration of the vehicle using the Markov chain according to the statistical information of driving condition data for the actual construction vehicle to ensure the prediction accuracy of the load torque demand. Second, considering the real time of the optimization solution, to avoid intense online computations, a scenario-based enumeration approach is used to solve a multistage stochastic optimization problem in the SMPC-EMS of the upper layer. Third, focusing on the nonlinear characteristics and uncertain parameters of the engine and external disturbance, an estimator of the total disturbance is combined with the MPC torque tracking controller of the engine in a closed-loop control of the lower layer to ensure the robustness of the tracking performance for the distributed torque from the upper-layer SMPC-EMS, and therefore the diesel engine operates quickly and stably in a high-efficiency fuel zone.

The remainder of this paper is organized as follows: The description of the studied system and the control problem are introduced in Section 2. Section 3 presents the design of the upper-layer SMPC energy management controller and the lower-layer engine fast speed tracking MPC controller are designed for the torque coupling system. The effectiveness and adaptability of the proposed method are verified using both simulation and the experiment test platform in Sections 4 and 5, respectively. In addition, the comparison results with the existing strategies are also presented. The conclusions of this paper are drawn in Section 6.

2. System Description and Control Problem

In a common spray-painting vehicle power system, the diesel engine directly matches the load torque demand of the main pump. The operation points of the engine probably enter the area with low fuel efficiency due to the frequent fluctuations of load. For fuel efficiency, a torque coupling structure using a secondary element hydraulic pump motor to adjust the engine torque output is a feasible power hybrid mode. For this study, the powertrain structure of a spray-painting vehicle is studied,

in which a single accumulator and a hydraulic bridge are used to achieve two-way energy collection instead of the hybrid structure of most HHVs using high and low pressure with two accumulators, as shown in Figure 1. In addition, for the secondary adjustment, the pressure coupling control commonly used in industrial control is introduced, therefore, the hydraulic pump/motor (PM) of the secondary adjustment component can respond quickly and achieves the purpose of rapid adjustment and energy saving. The diesel engine, hydraulic PM, and hydraulic main pump are connected to the transfer case with the transmission ratio 1:1:1, respectively. In the diesel hydraulic hybrid system, hydraulic energy is converted into mechanical energy through the hydraulic pump/motor and coupled with the energy output from the diesel engine to form a "torque coupling structure", and therefore it is a parallel HHV.
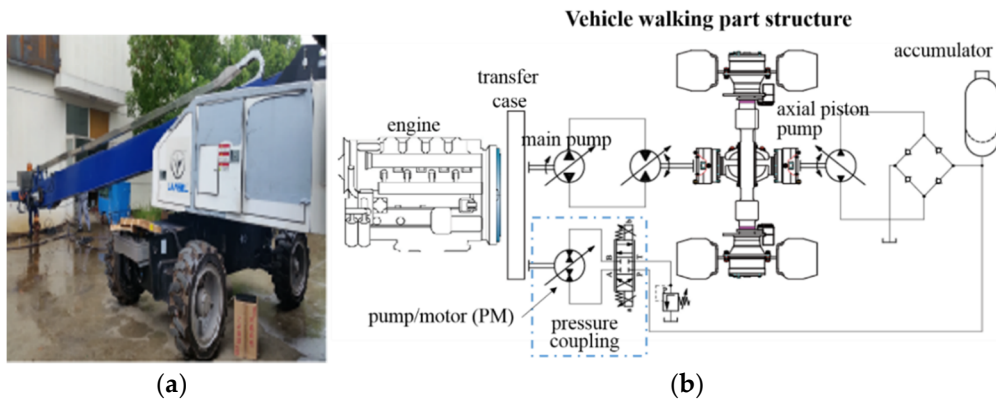
Figure 1. Powertrain system of a spray-painting vehicle: (**a**) A spray-painting vehicle and (**b**) sketch of the powertrain structure of a hybrid hydraulic vehicle (HHV).

The engine dynamic is described as follows:

$$J_e \dot{\omega}_e = T_e - T_{pm} - \frac{T_L}{\eta_p} - \mu \omega_e \tag{1}$$

where J_e is the rotational inertia, ω_e is the engine angular velocity, η_p is the efficiency of the main pump, μ is the friction coefficient, and T_e, T_{pm}, T_L represent engine torque, PM torque, and load torque, respectively, which are described as:

$$\begin{cases} T_e = f_e(\alpha_e, n_e) \\ T_{pm} = \frac{p_{pm} Q_{pm}}{2\pi n_e} \eta_{pm}^{sgn(Q_{pm})} \\ T_L = \left(\frac{C_d A v^2}{21.15} + f_r mg \cos\theta + mg \sin\theta + \delta m\dot{v} \right) r_w \end{cases} \tag{2}$$

where $n_e = \frac{30\omega_e}{\pi}$, α_e is the throttle opening angle of the engine; $f_e(\cdot, \cdot)$ is a nonlinear and empirical function of α_e and n_e, which is obtained by the surface fitting in Matlab toolbox; p_{pm}, Q_{pm}, η_{pm} are the pressure, flow, and efficiency of PM, respectively; C_d, f_r are air and rolling resistance coefficients, respectively; A, m, v are the frontal area, mass, and speed of vehicle, respectively; θ is the climbing angle; δ is a conversion factor of rotation mass; and r_w is the tire radius.

The fuel consumption rate of the diesel engine is calculated by the following relationship:

$$\dot{m}_f = \frac{T_e n_e}{9550} \cdot \frac{b_e(T_e, n_e)}{3600} \tag{3}$$

where b_e is the brake-specific fuel consumption, which can be obtained by a steady-state map of the engine speed and torque, shown in Figure 2 for a certain diesel engine.
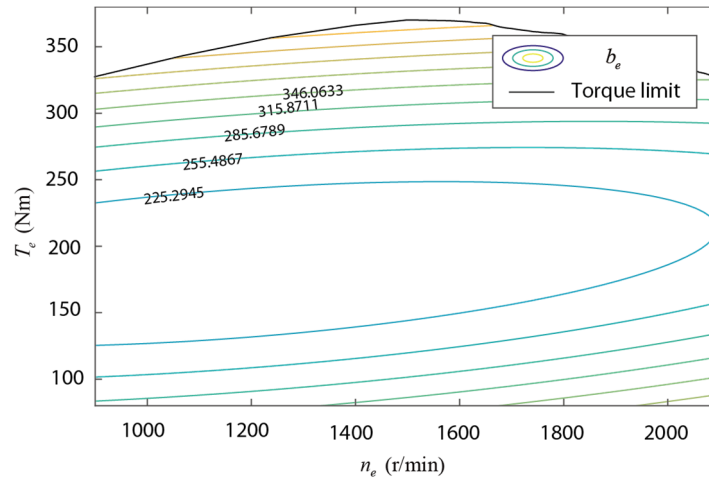
Figure 2. Brake-specific fuel consumption, b_e, map of the diesel engine.

When $T_L > 0$, the hydraulic unit is in an energy output state, and the traction torque is provided by the main pump. When $T_L < 0$, the vehicle is in a braking state, and the hydraulic unit does not provide energy. The flow of the axial piston pump when braking is:

$$Q_b = \eta_b \frac{V_b \cdot v}{2\pi r_w} \tag{4}$$

where η_b is the transmission ratio and V_b is the displacement of the axial piston pump.

According to Boyle's gas formula, the accumulator is modeled as follows:

$$\begin{cases} p_0 V_0^n = p_1 V_1^n = p_{acc} V_{acc}^n = \text{const} \\ SOC^* = -\int_{V_0}^{V_{acc}} p_{pm} dV = \frac{p_1 V_1^n}{1-n}[V_1^{1-n} - (V_1 - \Delta V)^{1-n}] \end{cases} \tag{5}$$

where p_0, V_0 denote the precharge pressure and volume of the accumulator, respectively; p_1 is the minimum working pressure; V_1 is the corresponding volume; p_{acc} and V_{acc} are the pressure and volume of the accumulator at any time; n is polytrophic exponent, here $n = 1.4$ [23]; and SOC^* is the energy of the accumulator. It can be seen from Equation (5) that when p_1 is determined, the SOC^* depends on hydraulic oil volume flowing into the accumulator ΔV.

Ignoring the loss of gas flow, the volume change in the accumulator is calculated as:

$$-\frac{dV}{dt} = Q_{pm} + Q_b \tag{6}$$

Thus, considering Equations (4) to (6), the accumulator power is characterized as:

$$\dot{SOC}^* = 2\pi T_{pm} n_e \eta_{pm}^{sgn(-T_{pm})} + \eta_b \frac{p_{pm} V_b v}{2\pi r_w} \tag{7}$$

It is worth mentioning that for simplifying the computation of the control design, the SOC^* is normalized as the state of charge (SOC) by defining

$$SOC = \frac{SOC^* - SOC^{*,\min}}{SOC^{*,\max} - SOC^{*,\min}} \tag{8}$$

with $SOC^{*,\min} = -\int_{V_0}^{V_{\min}} p_{pm} dV$, $SOC^{*,\max} = -\int_{V_0}^{V_{\max}} p_{pm} dV$, where V_{min} and V_{max} are the minimum and maximum volume of accumulator corresponding to the accumulator being empty and the accumulator being full [25], respectively. Accordingly, the SOC of the accumulator can be regarded as the ratio of the

variation of instantaneous fluid volume to the variation of maximum fluid capacity in the accumulator under certain pressures, and $SOC^{min} = 0$ and $SOC^{max} = 1$.

In the powertrain structure, as shown in Figure 1, hydraulic energy is converted into mechanical energy through a hydraulic PM coupled with the energy output from the diesel engine to form a torque coupling structure similar to a parallel HEV. Thus, by regulating the transfer of energy to/from the accumulator, the engine operates at its best operating zone to improve its fuel efficiency when it works. To achieve this, an appropriate EMS is necessary to allocate the demand of the load torque, and a satisfying tracking controller is necessary to ensure the desired output torque of the engine.

However, during the actual driving cycle of the construction vehicle, the driving style of the driver and the external environment, such as road type, slope, and other information, cause uncertain driving conditions with some randomness, which should be considered in the design of the EMS. Meanwhile, the uncertainty and nonlinearity of the engine dynamic and external disturbance should be taken into account in the design of the engine tracking controller. Consequently, a hierarchical control scheme, which can effectively deal with the randomness, uncertainty, and nonlinearity, are presented in this paper. The upper layer performs energy management to determine the energy distribution between the engine and the accumulator. The control objective is to minimize fuel consumption and ensure the control range of the SOC of the accumulator. The lower-layer controller is to ensure that the engine and the auxiliary power source operate at the desired operating zone based on the energy distribution result of the upper-layer.

3. MPC-Based Hierarchical Control Scheme

Considering uncertain driving conditions with some randomness in the energy distribution, and uncertainty and nonlinearity of the engine dynamic in the tracking control, an MPC-based hierarchical control structure is established for the HHV, as shown in Figure 3. The upper-layer is a SMPC-based EMS using the Markov prediction model for the torque demand in the finite horizon dealing with the uncertain driving conditions. The lower layer is a nonlinear MPC-based tracking controller with a disturbance estimator.
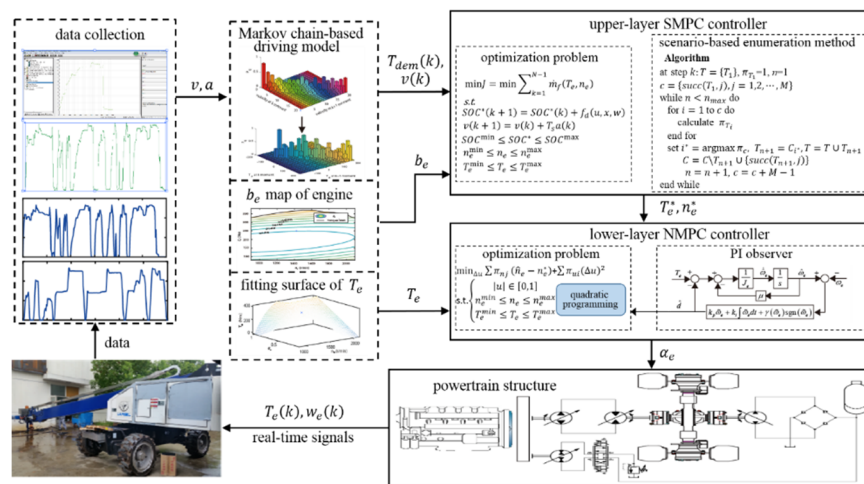

Figure 3. Sketch of the hierarchical control structure of HHV.

3.1. SMPC-Based Upper-Layer Energy Management Strategy Design

Similar to other normal driving vehicles, the spray-painting vehicle generates a series of acceleration and braking actions according to its driving intention and external environment, such as road type, slope, and road obstacles. These driving actions are uncertain random variables, which are random disturbances to the vehicle from outside. Therefore, the vehicle acceleration is regarded as a random variable, and the acceleration at the next moment is independent of the historical acceleration except for the current acceleration, and therefore the randomness satisfies the Markov characteristic. Accordingly,

the Markov model is built by estimating the transition probabilities that map the current acceleration to the next acceleration using the historical sample cycle data. Then, according to the relationship of the velocity, acceleration of the vehicle, and the torque demand, the prediction model of the torque demand is obtained, which is also a Markov-chain model in different velocities. The detail is stated as follows:

(1)   Using the collected cycle data and the sampling interval 20 ms, the maximum speed of the working condition 5.5 km/h, the maximum acceleration 0.08 m/s^2, and the minimum acceleration -0.12 m/s^2, the acceleration is discretized and pretreated to a positive integral value:

$$a \in a^1, a^2, \cdots a^M, \ (M = 21), \ a_{inte} = (a + 0.12) \times 100 = 0, 1, \cdots 20 \tag{9}$$

(2)   According to the maximum likelihood estimation method, the transition probability from the current acceleration $a_{inte,i}$ to the next moment acceleration $a_{inte,j}$ is calculated as:

$$P_{i,j} = P\left(a_{inte}(k+1) = a_{inte,j}\middle|a_{inte}(k) = a_{inte,i}\right) = \frac{F_{i,j}}{F_i}, \ F_i = \sum_{j=1}^{M} F_{i,j}, \ i, j = 1, 2, \cdots, M \tag{10}$$

where $F_{i,j}$ is the change number of the acceleration from $a_{inte,i}$ to $a_{inte,j}$ and F_i is the total transition number of $a_{inte,i}$. The estimated transition probabilities are shown in Figure 4.
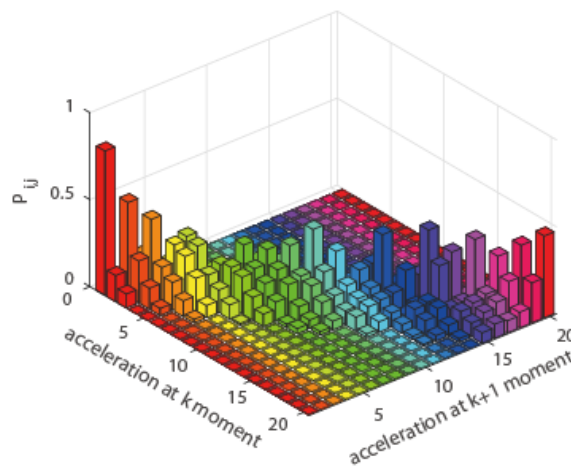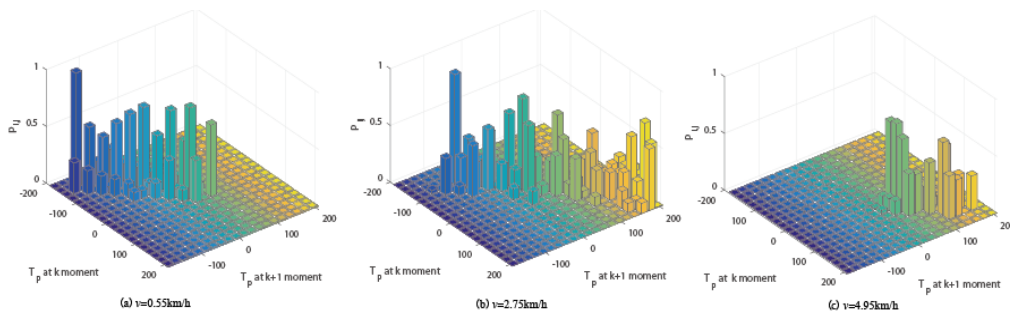

Figure 4. Transition probabilities of acceleration.

(3)   According to the established acceleration prediction model and the relationship of the velocity, acceleration of the vehicle and the torque demand are described as (1) and (2), i.e.,

$$\begin{cases} v(k+1) = v(k) + T_s a(k) \\ T_{dem}(k+1) = T_L/\eta_p = \left(\frac{C_d A v(k+1)^2}{21.15} + f_r mg \cos\theta + mg \sin\theta + \delta ma(k+1)\right) r_w/\eta_p \end{cases} \tag{11}$$

the prediction model of torque demand is obtained, as shown in Figure 5. It is also a Markov chain model in different velocities, which is used in the stochastic optimization of the following SMPC with finite receding horizon.

(a) v=0.55km/h (b) v=2.75km/h (c) v=4.95km/h

Figure 5. Transition probabilities of torque demand at different velocities.

According to the Markov prediction model, the SMPC problem is formulated, i.e., the moving horizontal optimization problem is solved as follows:

$$\min J = \min \sum_{k=1}^{N-1} \dot{m}_f(T_e(k), n_e(k)) \tag{12}$$

subject to the dynamic equation with the stochastic disturbance $w = [a, T_{dem}]^T$:

$$\begin{cases} SOC^*(k+1) = SOC^*(k) + 2\pi T_s(T_{dem}(k) - T_e(k))n_e\eta_{pm}^{sgn(-T_{pm}(k))} + \eta_b \frac{P_{pm}V_b}{2\pi r_w}v(k) \\ v(k+1) = v(k) + T_s a(k) \end{cases} \tag{13}$$

and the physical constrains for the state variable $x = [SOC^* \ v]^T$ and the control input $u = [T_e \ n_e]^T$:

$$\begin{cases} SOC^{\min} \leq SOC^* \leq SOC^{\max} \\ n_e^{\min} \leq n_e \leq n_e^{\max} \\ T_e^{\min}(n_e) \leq T_e \leq T_e^{\max}(n_e) \end{cases} \tag{14}$$

Recently, SMPC has been proposed and continues to evolve. The method utilizes statistical information of the disturbance to optimize the performance of a system as much as possible. This study used a scenario based on the SMPC method proposed in the literature [18]. The method is derived from the multistage stochastic optimization idea and uses stochastic models (such as Markov models) to describe the external random disturbances, and therefore improves the effect of model predictive control as much as possible. According to this feature, the Markov model proposed above can be conveniently applied to the method, and therefore the scenario based on the SMPC method is built using the updated information on the Markov chain (9) and (10), and system state.

- For predictive control based on a scenario stochastic model in the application process, it is necessary to predict the system state and disturbance in a future period (predicted time domain) from the current random disturbance and the measured value of the system state at each sampling moment. The predicted transient state of the system state and the disturbance interaction are also the so-called scenario. This scenario is used to predict the probability of reaching a node. Each node of the scenario represents a predicted state which is the weight factor in the optimization problem (14). This scenario is generally described in terms of trees, as shown in Figure 6, and this description method requires the introduction of the following variables and terms:
- $\Gamma = \{T_1, T_2, \cdots, T_n\}$, the set of the tree nodes. Nodes are indexed progressively as they are added to the tree (i.e., T_1 is the root node and T_n is the last node added);
- $pre(T) \in \Gamma$, the predecessor of the node T;
- $succe(T, j) \in \Gamma$, the successor of node T with value $a_{inte,j}$;
- x_T, u_T, w_T, the state, the output and the disturbance, respectively, associated with node T, where $x_{T_1} = x(k)$ and $w_{T_1} = w(k)$;

- $\pi_T \in [0,1]$, the probability of reaching node T (from T_1);
- $C = \{C_1, C_2, \cdots, C_c\}$, the set of candidate nodes, defined as $C = \{T \notin \Gamma | \exists (i,j) : T = succ(T_i, j)\}$;
- $S \subset \Gamma$, the set of leaf nodes, $S = \{T \in \Gamma | succ(T,j) \notin \Gamma, \; \forall j \in \{1, 2, \cdots, M\}\}$.
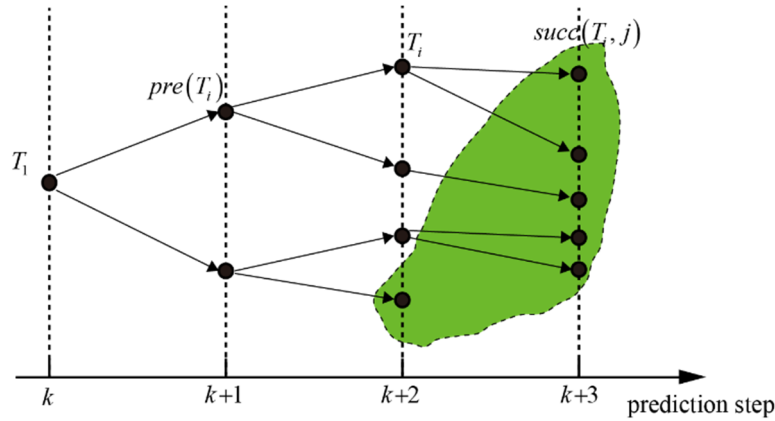

Figure 6. Optimization tree diagram.

Every route from root node to leaf node presents a disturbance scenario that is considered in the optimization problem, a list of possible candidates is evaluated, and the node with largest realization probability is added to the tree until a desired number of nodes, n_{max}, is reached. The procedure to construct scenario tree is listed in the following Algorithm 1:

Algorithm 1 SMPC Scenario Tree Generation Procedure

At any step k: set $\Gamma = \{T_1\}$, $\pi_{T_1} = 1$, $n = 1$, $c = \{succ(T_1, j), \; j = 1, 2, \cdots, M\}$. $(k = 1, \ldots, N-1)$

while $n < n_{max}$ do

For $i = 1$ To c Do

Calculate π_{T_i} according to (10) and (11)

End for

Set $i^* = \arg \max\limits_{i \in \{1, \cdots, c\}} \pi_{C_i}$, $T_{n+1} = C_{i^*}$, $T = T \cup (T_{n+1})$,

$\quad C = C \backslash T_{n+1} \cup \{succ(T_{n+1}, j)\}$, $j = 1, 2, \cdots, M$, $n = n+1$, $c = c + M - 1$.

End while

In addition, in order to prevent large changes in the SOC of the accumulator at the beginning and the end of the cycle, energy constraint for the accumulator at the initial and final values is added into the cost function of the optimization.

According to (12) to (14), the SMPC problem at time k is formulated as:

$$\min_u \sum_{i \in \Gamma \backslash \{T_1\}} \pi_{T_i} Q \left(SOC_{T_i} - SOC_{ref} \right)^2 + \sum_{i \in \Gamma \backslash S} \pi_{T_i} R \dot{m}_f^2 \left(u_{T_i} \right)$$

$$s.t. \begin{cases} x_{T_1} = x(k) \\ x_{T_i} = f \left(x_{pre(T_i)}, u_{pre(T_i)}, w_{T_i} \right), T_i \in \Gamma \backslash \{T_1\} \\ SOC^{min} \leq SOC_{T_i} \leq SOC^{max}, \; T_i \in \Gamma \backslash \{T_1\} \\ u^{min} \leq u_{T_i} \leq u^{max}, \; T_i \in \Gamma \backslash S \end{cases} \tag{15}$$

where Q and R are nonnegative scalar weights, problem (15) can be cast as a standard quadratic programming problem (QP).

3.2. MPC-Based Lower-Layer Engine Speed Tracking Controller Design

Considering the nonlinear system characteristics of the engine, an MPC controller is designed to obtain better performance of setpoint tracking of engine torque. The speed regulation characteristic model of the diesel engine, i.e., the quadratic function T_e on (n_e, α_e) is shown in Figure 7.
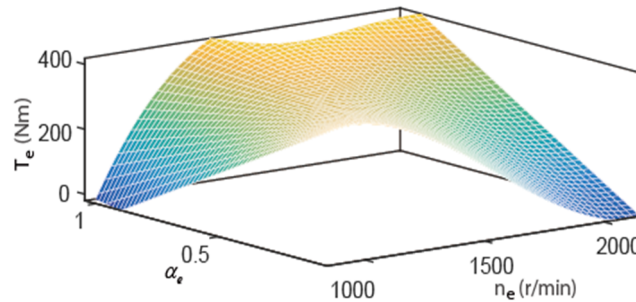

Figure 7. Speed regulation characteristic model of the engine.

Using the surface fitting in Matlab toolbox function, the following expression can be obtained:

$$
\begin{aligned}
T_e = f_e(n_e, \alpha_e) &= 5.996n_e^3 - 15.04n_e^2 - 9.35n_e^2\alpha_e - 7.59n_e\alpha_e - 22.29n_e + 50.44\alpha_e + 349.5 \\
&= \sum_{l=0}^{3} c_l n_e^l + \sum_{m=0}^{2} c_m n_e^m \alpha_e
\end{aligned}
\tag{16}
$$

Combining (1), (2), and (16), and Euler discretization, the dynamic of engine is described as:

$$
\begin{cases}
n_e(k+1) = a_1 n_e(k) + a_2 \sum\limits_{l=0}^{3} c_l n_e^l(k) + a_2 \sum\limits_{m=0}^{2} c_m n_e^m(k)u(k) + d \\
y(k) = n_e(k)
\end{cases}
\tag{17}
$$

where $a_1 = 1 + T_L \mu a_2 / \eta_p$, $a_2 = T_L 30 / (j_e \pi \eta_p)$, and $d = T_L a_2 (T_{pm} + T_p) / \eta_p$, $u = \alpha_e$.

At the step k, the one-step prediction of the system (17) is:

$$
\begin{aligned}
\hat{n}_e(k+1 \mid k) &= a_1 n_e(k|k) + a_2 \sum_{l=0}^{3} c_l n_e^l(k|k) + a_2 \sum_{m=0}^{2} c_m n_e^m(k|k)(u(k-1) + \Delta u(k)) + \hat{d} \\
&= G_0(n_e(k|k), u(k|k)) + \hat{d}
\end{aligned}
\tag{18}
$$

where the control input $u(k|k) = u(k-1) + \Delta u(k)$ at step k, $u(k-1)$ is the known last step input and $\hat{d}$ is the observation of d, which is introduced later. Similarly, at time k the N-step prediction could be obtained by step-ahead iterative method.

$$
\begin{aligned}
\hat{n}_e(k+2|k) &= G_0(k+1|k, u(k+1|k)) + \hat{d} \\
&= G_1(n_e(k|k), u(k|k), u(k+1|k)) + \hat{d}, \\
&\vdots \\
\hat{n}_e(k+j|k) &= G_{j-1}(n_e(k|k), u(k|k), \cdots, u(k+j-1|k)) + \hat{d}.
\end{aligned}
\tag{19}
$$

The moving horizontal optimization control problem is for the reference signals $n_e^*(k+1\,|\,k), n_e^*(k+2\,|\,k), \cdots$, which is distributed through the upper-layer EMS, to find a feedback control law $\Delta u(k)$ of every predictive step such that:

$$\min_{\Delta u} \sum_{j=1}^{N} \pi_{nj}\left(\hat{n}_e(k+j|k) - n_e^*(k+j\,|\,k)\right)^2 + \sum_{i=1}^{P} \pi_{ui}(\Delta u(k))^2$$

$$s.t.\begin{cases} 0 \le |u(k)| \le 1 \\ 0 \le |\Delta u(k)| \le 1 \\ n_e^{\min} \le n_e \le n_e^{\max} \\ T_e^{\min} \le T_e \le T_e^{\max} \end{cases} \tag{20}$$

where N is the prediction time domain, P is the control time domain, π_{nj} and π_{ui} are the weight coefficients and, at this point, the engine speed tracking control problem is transformed into a multi-constrained quadratic programming problem, which can be solved by the self-embedded "fmincon" of MATLAB software.

In (17), d contains the torques of load and PM, T_L is an unmeasurable variable in actual engineering, therefore, an observer needs to be designed to estimate it and (1) is rewritten as follows:

$$J_e \dot{\omega}_e = T_e - \mu \omega_e - d \tag{21}$$

Assumption $d = d_0$ at $k - 1$ time, then the actual d can be described at time k as follow:

$$d = d_0 + \Delta(\widetilde{\omega}_e) \tag{22}$$

where $\Delta(\widetilde{\omega}_e)$ is an unknown function that is bounded by a known function $\gamma(\widetilde{\omega}_e)$. On the basis of the principle of PI observer in Figure 3, the observer can be formulated as follows:

$$\begin{cases} \hat{d} = k_p\widetilde{\omega}_e + k_i \int \widetilde{\omega}_e dt + \gamma(\widetilde{\omega}_e)\mathrm{sgn}\widetilde{\omega}_e \\ \dot{\hat{\omega}}_e = \frac{1}{J_e}\left(T_e - \mu\hat{\omega}_e - \hat{d}\right) \end{cases}, \tag{23}$$

4. Simulation Validation Results

In order to evaluate the performance of the proposed hierarchical MPC, a high-fidelity simulation model of HHV is built in Matlab/Simulink. Using a spray-painting vehicle as a research platform, a torque coupled HHV model, as shown in Figure 1, is constructed, and the actual physical parameters are listed in Table 1.

Table 1. Spray-painting vehicle parameters.

Notation	Meaning	Unit	Value
m	vehicle mass	kg	18,000
v_{max}	maximum vehicle speed	km/h	5.5
A	frontal area of vehicle	m^2	8.3
C_d	air resistance coefficient		0.58
δ	rotation mass conversion factor		1.065
f_r	rolling resistance coefficient		0.0135
P_{emax}	maximum power of diesel engine	kW	88
r_w	the tire radius	m	0.375

Several driving cycles are considered for simulation verification, which belong to the database that is used to predict vehicle v^* and torque demand T_{dem} by Markov chain offline calculations.

One of the driving conditions, namely the first driving condition, is considered, which is shown in Figure 8, and the calculated v^* and T_{dem} through the Markov model are also shown. In the first two graphs of Figure 8, the red dotted line is the predicted vehicle speed and torque demand using the

one-step Markov model and (11), respectively, the predicted time domain is 1 s and the corresponding root mean square error of acceleration is 0.3267. In addition, the predicted time domain length is 3 s, 5 s, and 10 s, respectively. The speed and torque demand are also predicted by the one-step Markov model. By contrast, as the prediction zone increases, the root mean square error becomes larger and larger, indicating that the prediction accuracy is less. On the one hand, the Markov process is random, and the prediction of each step only roughly reflects the change of speed, so there is an error in the prediction result. On the other hand, in the process of using the Markov model for prediction, the predicted speed at the previous moment is used as the initial acceleration predicted at the next moment, thereby superimposing the error on the next stage. Therefore, the longer the prediction zone, the more times the error is superimposed, and the less accurate the predicted power demand. The third and fourth graphs of Figure 8 are the mileage and the height of the road during driving, which calculate fuel consumption and slope.
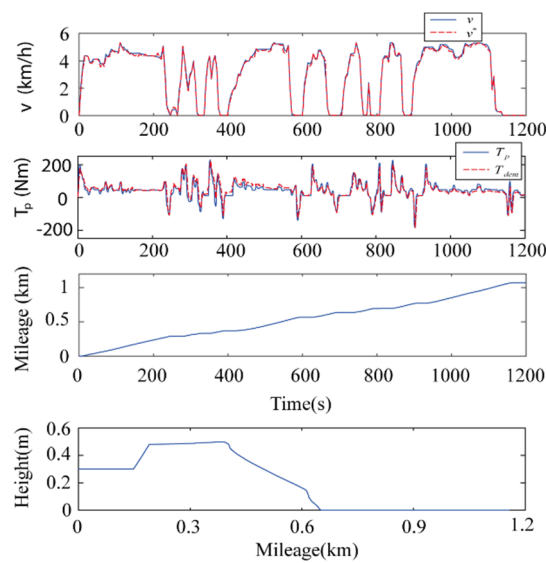

Figure 8. First driving conditions.

Simulation verification for the upper-layer EMS is first performed according to the first driving condition. Setting the initial value of state input $SOC_0 = 0.6$, $SOC_{ref} = 0.6$, $n_{e0} = 900$ r/min, and $T_{e0} = 0$ Nm, the optimization tree is built with nodes $n_{max} = 50$.

To completely verifying the effectiveness and advantage of the proposed EMS, the comparisons among four EMSs are presented, which include the SMPC proposed in this study, a prescient MPC (PMPC) that knows the future torque request along the entire prediction horizon, a rule-based (RB) method proposed in [4], and a SDP algorithm designed in [26]. Therefore, the four EMSs are applied in the upper-layer EMS to carry out the distribution of the power demand, respectively. It should be noted that the simulation operation is carried out under the closed-loop control for the whole HHV, thus, in the simulation verification, one of the four EMSs is used in the upper layer, meanwhile, the designed MPC tracking controller of the engine is also embedded into the lower layer. The simulation results are shown in Figure 9.
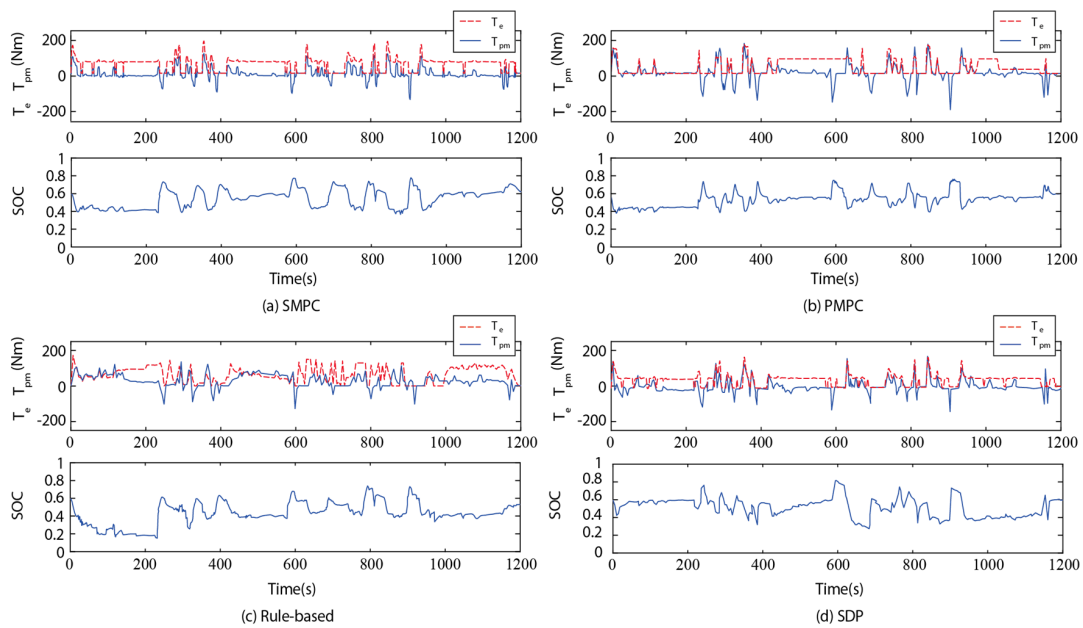
Figure 9. Simulation results of upper-layer energy management control strategy (EMS) under the first conditions.

Moreover, to verify the effectiveness of the designed lower layer controller, the comparison results are presented between the designed MPC tracking controller and a PID controller of the conventional engineering control method. Consequently, in the simulation verification, the designed SMPC, RB, and SDP EMSs are used in the upper layer, respectively, and the designed MPC tracking controller and a PID controller are embedded into the lower layer, respectively. The simulation comparison results are shown in Figure 10.
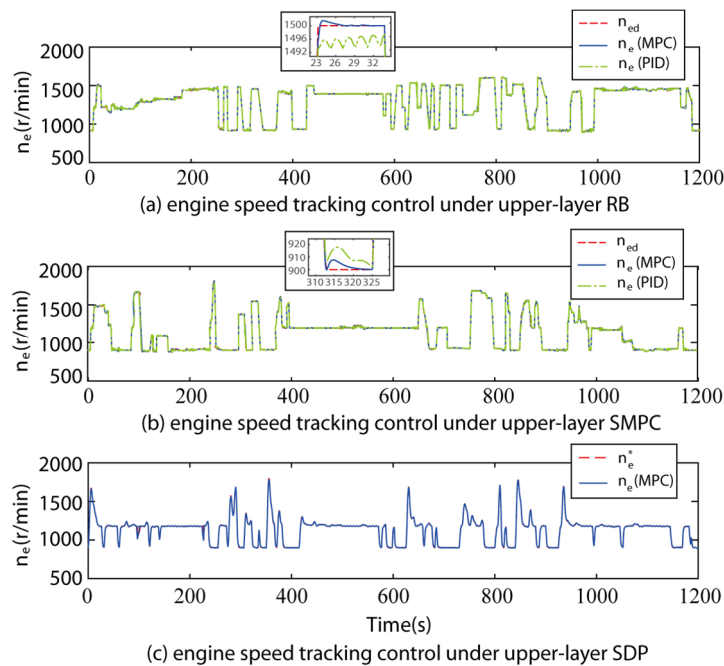
Figure 10. Lower-layer engine speed tracking control under the first conditions.

To facilitate comparative analysis of the control performance of various strategies, the simulation results are summarized, as listed in Table 2, where the different control strategies include: only PID lower-layer control for the conventional diesel engine driving construction vehicle (without

SOC); the upper-layer RB and the lower-layer PID that are adopted in practice (RB+PID), as well as the upper-layer RB and the lower-layer MPC (RB+MPC), the upper-layer SDP and the lower-layer MPC (SDP+MPC), the upper-layer SMPC and the lower-layer PID (SMPC+PID), the upper-layer SMPC and the lower-layer MPC (SMPC+MPC); and the upper-layer PMPC, and the lower-layer MPC (PMPC+MPC) for the benchmark. The evaluated control performance contains the final SOC, the variation range of SOC during the driving cycle, and the fuel economy expressed by miles per gallon (mpg). It is worth mentioning that although the final SOC is not the same for different control strategies, the corresponding fuel consumptions theoretically can be compared directly with each other due to very low accumulator capacity and the close final SOC of various strategies.

Table 2. Simulation comparison of different algorithms in the first driving conditions.

EMS+Engine Control	Final SOC Value	SOC Range	Fuel Economy (mpg)
+PID (without SOC)	-	-	31.74
RB+PID (practice)	0.587	0.19–0.76	34.63
RB+MPC	0.587	0.19–0.76	35.43
SDP+MPC	0.603	0.29–0.80	37.48
SMPC+PID	0.593	0.39–0.80	37.39
SMPC+MPC (proposed)	0.593	0.39–0.80	38.21
PMPC+MPC (benchmark)	0.603	0.40–0.79	39.24

From Table 2, it can be seen that at the end of the driving cycle, the SOC of the accumulator of all strategies is between 0.58 and 0.61, which means the energy of the accumulator is balanced. In addition, because a bladder accumulator is used, in order to extend the life of the bladder during the working process, it is necessary to avoid the contraction and expansion of the bladder from colliding with the bacteria valve at the lower end of the accumulator. From the variation range of SOC, various strategies meet the requirements for use. Fuel economy is the most concerned evaluation index of energy management strategy. It can be seen from Table 2 that compared with traditional engineering vehicles (without SOC), when the upper-layer control adopts the RB strategy (RB+PID), the fuel economy is improved by 9.1%, whereas when the lower-level controller uses the designed MPC tracking controller in this study instead of the PID controller (RB+MPC), fuel economy is further improved by 2.3%. Furthermore, when the upper layer uses the SDP (SDP+MPC) and the proposed SMPC (SMPC+MPC), the fuel economy is improved by 5.8% and 7.8% as compared with the RB+MPC strategy, respectively. Fuel economy of the PMPC+MPC strategy increases by 10.7% as compared with the RB+MPC strategy. It is worth mentioning that in the PMPC control strategy the entire driving conditions are regarded as completely known and the optimization solution is obtained by the DP, which is impossible to implement in practice and, in this study, is listed only for the benchmark. Therefore, from these results, we concluded that the proposed SMPC-EMS had much superiority in fuel economy. In addition, as compared with the SMPC+PID, the fuel economy of the SMPC+MPC is further improved by 2.2%. This result, together with the comparison between the RB+MPC and the RB+PID, means that the designed MPC tracking controller of the lower layer has an indelible contribution to fuel economy.

In order to verify the performance of the controller under different driving conditions and prediction biases, another driving cycle, shown in Figure 11, is also considered in simulation, which does not belong to the database used to predict vehicle and torque demand by Markov chain offline calculations. The corresponding prediction information is based on the Markov model. Moreover, according to simulation results, the root mean square error of the prediction speed based on the Markov model is 0.5743 when the predicted time domain length is 1 s, which is larger than that of the first driving cycle.
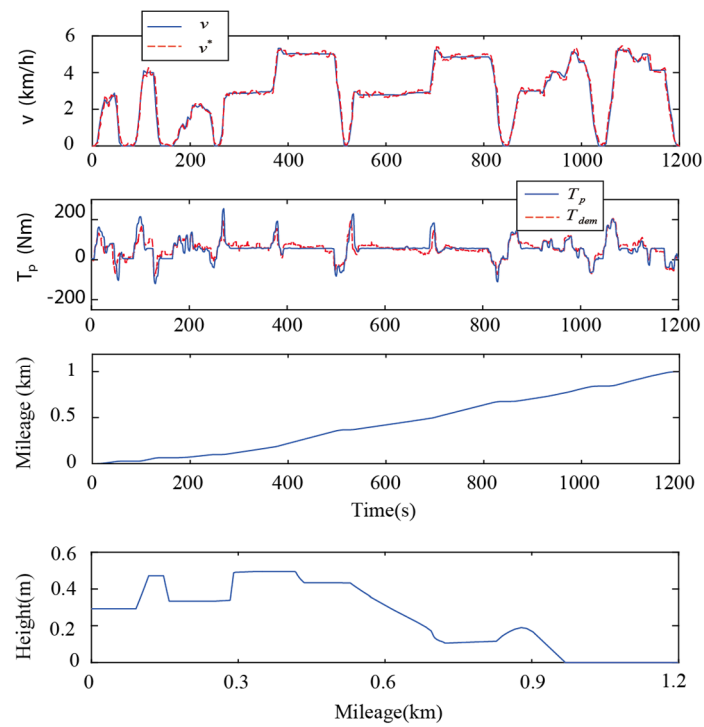
Figure 11. Second driving conditions.

Similar to the first driving conditions, Figure 12 shows the simulation results for different upper-layer EMSs for the second driving conditions. Figure 13 shows the simulation results of the comparisons among the RB+PID, RB+MPC, SMPC+MPC, SMPC+PID, and SDP+MPC. Table 3 lists the simulation results in the second driving conditions.
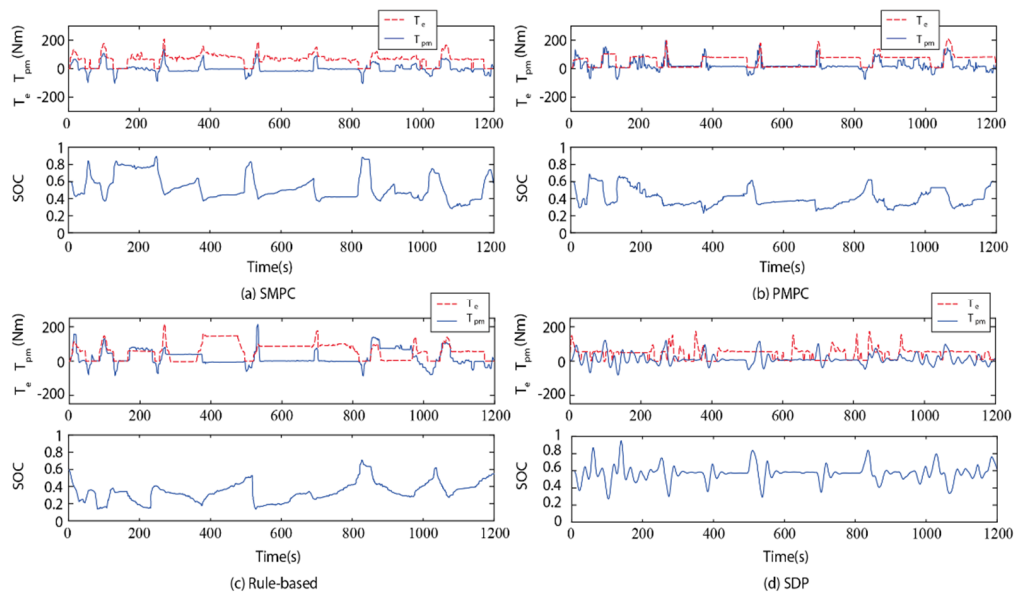

Figure 12. Simulation results of different upper-layer EMS in the second driving conditions.
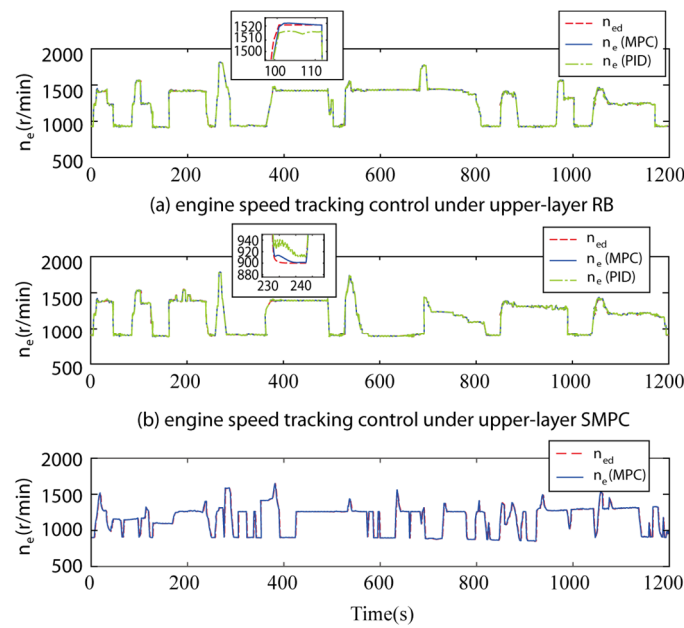
Figure 13. Lower-layer engine speed tracking control in the second driving conditions.

Table 3. Simulation comparison of different algorithms in the second driving conditions.

EMS+Engine Control	Final SOC Value	SOC Range	Fuel Economy (mpg)
+PID (without SOC)	-	-	31.82
RB+PID (practice)	0.592	0.18–0.69	34.43
RB+MPC	0.592	0.18–0.69	35.15
SDP+MPC	0.608	0.21–0.82	37.18
SMPC+PID	0.607	0.37–0.90	36.26
SMPC+MPC (proposed)	0.607	0.37–0.90	37.85
PMPC+MPC (benchmark)	0.602	0.39–0.82	38.89

From Table 3, it can be seen that the final value of SOC has basically returned to the initial value, and the working range of SOC meets the actual use environment, and there is no case of bladder contraction or expansion. In the hybrid hydraulic system, fuel economy is greatly improved by implementing different optimization strategies under the constraint conditions, in which the rule-based control strategy is improved by 11.3%. Accordingly, the PMPC method that is used as a performance benchmark, further improved by 9.76%. In addition, fuel economy is improved by 6.8% and 4.9% as compared with RB strategy, respectively, using the upper-layer EMS of SMPC and SDP based on the deviations predicted by the same Markov model. This shows that even if the predicted deviation of demand torque is large, SMPC still has better adaptability to driving condition to achieve a significant increase in fuel economy. In addition, the strategy of adopting MPC in the lower-layer controller still has a certain effect on the improvement of fuel economy as compared with the PID control method.

5. Experimental Evaluation

In the section, the proposed control strategy is verified by the experimental results carried out on a test platform indoors, as shown in Figure 14. The test platform consists of a power distribution unit, a load unit, and a control unit, where the electric motor is adjusted by the inverter to simulate the engine torque, and the load unit simulates the load torque by adjusting the pump pressure.
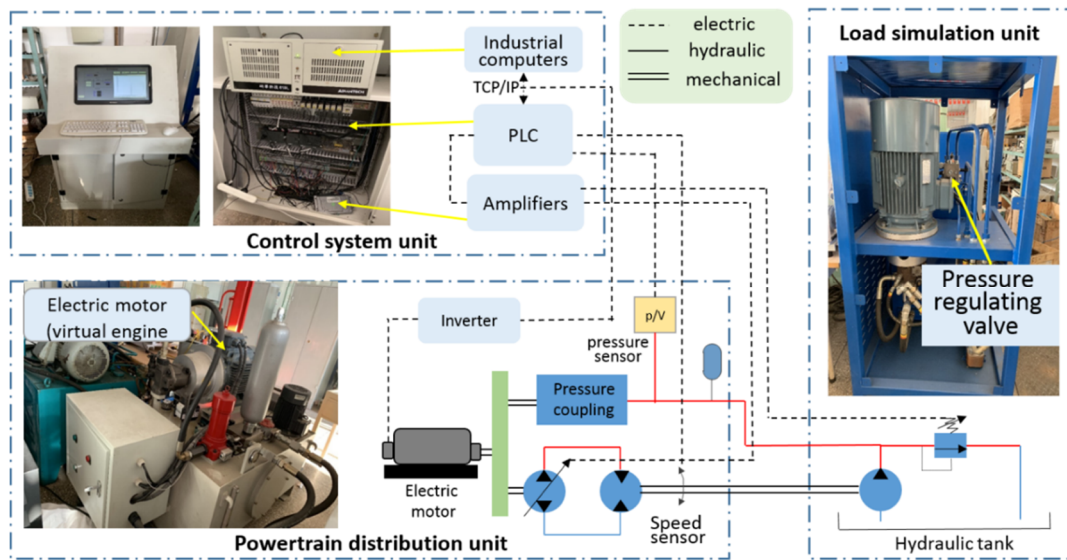
Figure 14. Structure of experiment platform.

The main parameters of the powertrain system on the test platform are shown in Table 4.

Table 4. Powertrain system parameters.

System Components	Parameter/(Uint)	Value
Electric motor (virtual engine)	rated power/(kW)	30
Main pump	flow/(ml/r)	28
	max pressure/(Mpa)	30
Hydraulic motor	flow/(ml/r)	28
	max pressure/(Mpa)	30
accumulator	rated volume/(L)	18.9
	working pressure/(Mpa)	[8,30]
	precharge pressure/(Mpa)	5.5

The experiment process is briefly described below. First, the load, T_p, of the entire vehicle is simulated by adjusting the pressure of the load unit to form the torque demand that is distributed by the EMS of the upper layer. The experimental data is obtained by PLC collecting sensors installed on the experimental platform. However, during the experiment, the electric motor only simulates the engine torque, therefore the fuel consumption is obtained by querying the Map table through the actual torque of the electric motor.

The first driving conditions are considered in the experiment and three EMSs of the upper layer including the RB, the SDP, and the SMPC are carried out on the test platform, respectively. The experimental results are shown in Figure 15. Meanwhile, Table 5 shows the evaluation performance for the experimental results of the three EMS strategies.
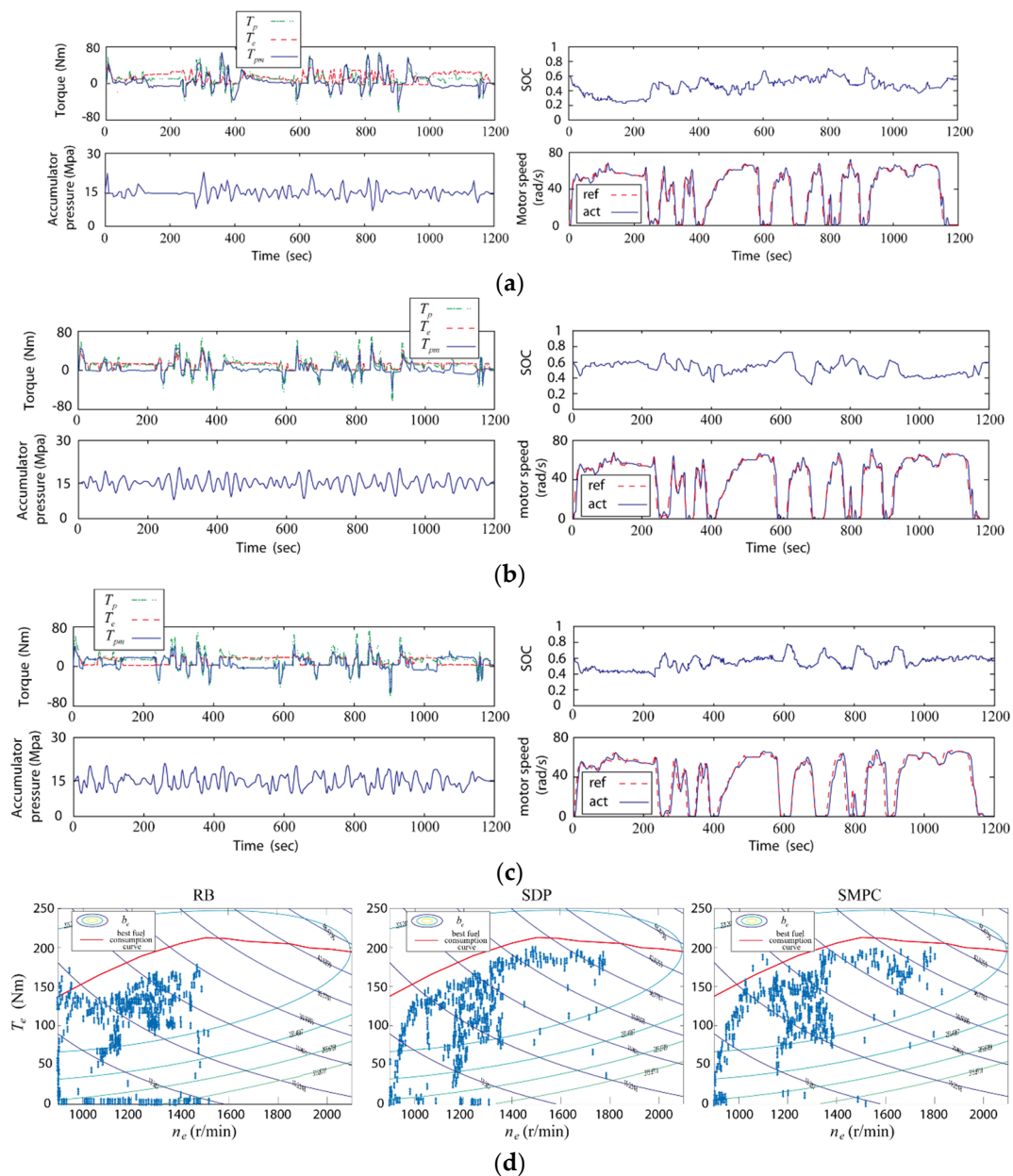
Figure 15. Experimental results of three control strategies: (**a**) Results for the rule-based strategy, (**b**) results for SDP strategy, (**c**) results for SMPC strategy, and (**d**) comparison of engine operating points under three EMS.

Table 5. Experimental results.

Parameters (unit)	RB	SDP	SMPC
Accumulator pressure range (MPa)	8.5–22.5	9.1–20.8	9.1–20.3
Final SOC value	0.583	0.603	0.605
SOC range	0.22–0.65	0.34–0.76	0.39–0.77
Motor speed bias (rad/s)	4.9	5.1	5.2
Fuel economy (mpg)	33.62	34.98	35.61

It can be seen from Table 5 and Figure 15:

1. Three EMS control strategies can satisfy the pressure of the accumulator within the working range. The SOC value meets the work requirements. The range of SOC value changes is significantly

smaller as compared with the simulation results. This is because the leakage of the pipeline is not considered in the system model.

2. It can be observed that the SMPC strategy has better fuel economy than the SDP and RB strategies. The SMPC and SDP methods have improved fuel economy by 5.9% and 4%, respectively as compared with the RB strategy. This verifies the effectiveness and advantage of the proposed method.

3. By comparing the speed tracking deviation of the hydraulic motor, the optimization-based EMS is slightly larger than the RB strategy. This is because the method based on the optimization strategy has a large calculation amount, which makes the control system have a certain delay.

On the basis of the aforementioned analysis, the proposed control strategy, in this study effectively improved the fuel economy of torque-coupled HHVs, on the premise that the vehicle performance requirements were met.

6. Conclusions

In this study, a hierarchical model predictive control was developed for torque-coupled HHVs in order to further improve fuel economy in the presence of the relatively low energy density of the hydraulic accumulator and frequent load changes, the randomness of the driving conditions, and the uncertainty of the engine dynamics. The proposed control is comprised of a SMPC-EMS in the upper layer and an MPC tracking controller for the engine in the lower layer. The SMPC-EMS is designed using a Markov prediction model and scenario-based enumeration approach, and the MPC tracking controller is combined with a load observer. Simulation verification and comparisons were performed for two driving conditions. Meanwhile, the experimental validation carried out on the test platform was also presented. The main findings of this work can be summarized as follows:

1. The EMS of the upper layer has a direct influence on the improvement of fuel economy. The optimization-based EMS has better fuel economy than the RB-EMS, which was proved by an average increase of 5.4% and 7.3% for the SDP and the SMPC, respectively, in the simulation results, and an increase of 4.0% and 5.9% for the SDP and the SMPC, respectively, in the experimental results.

2. In the optimization-based EMS, both close to globally optimal and online implementable EMS have the advantage of further improvement in fuel economy. In the proposed SMPC-EMS, the Markov prediction model and online regulation of MPC ensured the adaptability to driving conditions and the accuracy of the torque demand distribution, which results in a further increase of fuel economy than the offline optimization-based SDP.

3. The closed-loop controller of the lower layer has an indelible contribution to fuel economy, and a well-designed controller ensures the tracking performance of the distribution torque from the EMS of the upper layer, and therefore further improvements the fuel economy. This was evidenced by an increase of 2.3% for the RB+MPC as compared with the RB+PID, and an increase of 2.2% for the SMPC+MPC as compared with the SMPC+PID.

4. From the experimental results, we found that, in practice, the optimization calculation amount of the optimization-based EMS could influence the control performance. Therefore, in future work, we should find ways to further reduce optimization calculation and increase the calculation speed of the control system in the design of EMS.

Author Contributions: Z.W. wrote the original draft, designed control method, drew the figures and carried out the simulations; X.J. was responsible for supervising and guiding this research and reviewed and revised the article draft. All authors have read and agreed to the published version of the manuscript.

Conflicts of Interest: The authors declare no conflicts of interest.

References

1. Taymaz, I.; Benli, M. Emissions and fuel economy for a hybrid vehicle. *Fuel* **2014**, *115*, 812–817. [CrossRef]
2. Niu, G.; Shang, F.; Krishnamurthy, M.; Garcia, J.M. Design and analysis of an electric hydraulic hybrid powertrain in electric vehicles. *IEEE Trans. Transp. Electr.* **2017**, *3*, 48–57. [CrossRef]
3. Chen, Y.-L.; Liu, S.-A.; Jiang, J.-H.; Shang, T.; Zhang, Y.-K.; Wei, W. Dynamic analysis of energy storage unit of the hydraulic hybrid vehicle. *Int. J. Automot. Technol.* **2013**, *14*, 101–112. [CrossRef]
4. Hippalgaonkar, R.; Ivantysynova, M. Optimal power management of hydraulic hybrid mobile machines—Part I: Theoretical studies, modeling and simulation. *J. Dyn. Syst. Meas. Control.* **2016**, *138*, 051002. [CrossRef]
5. Zhang, W.; Wang, J.; Du, S.; Ma, H.; Zhao, W.; Li, H. Energy management strategies for hybrid construction machinery: Evolution, classification, comparison and future trends. *Energies* **2019**, *12*, 2024. [CrossRef]
6. Wang, D.; Guan, C. Optimal Control for a parallel hybrid hydraulic excavator using particle swarm optimization. *Sci. World J.* **2013**. [CrossRef] [PubMed]
7. Kamal, E.; Adouane, L. Hierarchical energy optimization strategy and its integrated reliable battery fault management for hybrid hydraulic-electric vehicle. *IEEE Trans. Veh. Technol.* **2018**, *67*, 3740–3754. [CrossRef]
8. Wang, Z.; Jiao, X.; Pu, Z.; Han, L. Energy recovery and reuse management for oil-electric-hydraulic hybrid powertrain of construction vehicle. *IFAC Pap. Online* **2018**, *51*, 390–393. [CrossRef]
9. Gong, J.; Zhang, D.; Guo, Y.; Liu, C.; Zhao, Y.; Hu, P.; Quan, W. Power control strategy and performance evaluation of a novel electro-hydraulic energy-saving system. *Appl. Energy* **2019**, *233–234*, 724–734. [CrossRef]
10. Vu, T.V.; Vu, T.H. An improvement of rule-based control strategy for a series hydraulic hybrid vehicle. In *Recent Advances in Electrical Engineering and Related Sciences, Lecture Notes in Electrical Engineering*; Springer: Gewerbestrasse, Cham, Switzerland, 2017; Volume 415, pp. 902–912. [CrossRef]
11. Wu, B.; Lin, C.-C.; Filipi, Z.; Peng, H.; Assanis, D. Optimal power management for a hydraulic hybrid delivery truck. *Veh. Syst. Dyn.* **2004**, *42*, 23–40. [CrossRef]
12. Chen, C.-K.; Vu, T.-V.; Hung, C.-W. A simulation study of power management for a series hydraulic hybrid vehicle. In *Recent Advances in Electrical Engineering and Related Sciences, Lecture Notes in Electrical Engineering*; Springer: Berlin/Heidelberg, Germany, 2014; Volume 282, pp. 413–422. [CrossRef]
13. Chen, Q.; Lin, T.; Ren, H. Parameters optimization and control strategy of power train systems in hybrid hydraulic excavators. *Mechatronics* **2018**, *56*, 16–25. [CrossRef]
14. Zhou, H.; Zhao, P.-Y.; Chen, Y.-L.; Yang, H.-Y. Prediction-based stochastic dynamic programming control for excavator. *Autom. Constr.* **2017**, *83*, 68–77. [CrossRef]
15. Kim, H.; Yoo, S.; Cho, S.; Yi, K. Hybrid control algorithm for fuel consumption of a compound hybrid excavator. *Autom. Constr.* **2016**, *68*, 1–10. [CrossRef]
16. Deppen, T.O.; Alleyne, A.G.; Stelson, K.; Meyer, J. An energy management strategy for a hydraulic hybrid vehicle. In Proceedings of the 2012 American Control Conference (ACC), Montréal, Canada, 27–29 June 2012; pp. 1335–1341. [CrossRef]
17. Bender, F.A.; Kaszynski, M.; Sawodny, O. Drive cycle prediction and energy management optimization for hybrid hydraulic vehicles. *IEEE Trans. Veh. Technol.* **2013**, *62*, 3581–3592. [CrossRef]
18. Bender, F.A.; Kaszynski, M.; Sawodny, O. Location-based energy management optimization for hybrid hydraulic vehicles. In Proceedings of the 2013 American Control Conference, Washington DC, USA, 17–19 June 2013; pp. 402–407. [CrossRef]
19. Karbaschian, M.A.; Söffker, D. Toward On-Line Optimized Power Management for a Series Hybrid Hydraulic Powertrain. In Proceedings of the 2014 IEEE Vehicle Power and Propulsion Conference (VPPC), Coimbra, Portugal, 27–30 October 2014; pp. 1–6. [CrossRef]
20. Deppen, T.O.; Alleyne, A.G.; Stelson, K.; Meyer, J. A model predictive control approach for a parallel hydraulic hybrid powertrain. In Proceedings of the 2011 American Control Conference, San Francisco, CA, USA, 29 June–1 July 2011; pp. 2713–2718. [CrossRef]
21. Feng, D.; Huang, D.; Li, D. Stochastic model predictive energy management for series hydraulic hybrid vehicle. In Proceedings of the 2011 IEEE International Conference on Mechatronics and Automation, Beijing, China, 7–10 August 2011; pp. 1980–1986. [CrossRef]
22. Karbaschian, M.A.; Söffker, D. Application and Comparison of Pressure Control Strategies to a Series Hybrid Hydraulic Powertrain. In Proceedings of the 2014 IEEE Vehicle Power and Propulsion Conference (VPPC), Coimbra, Portugal, 27–30 October 2014; pp. 1–6. [CrossRef]

23.　Vu, T.-V.; Chen, C.-K. A model-based controller development for a series hydraulic hybrid vehicle. In *Recent Advances in Electrical Engineering and Related Sciences, Lecture Notes in Electrical Engineering*; Springer: Gewerbestrasse, Cham, Switzerland, 2017; Volume 415, pp. 891–901. [CrossRef]

24.　Zeng, X.; Li, G.; Yin, G.; Song, D.; Li, S.; Yang, N. Model predictive control-based dynamic coordinate strategy for hydraulic hub-motor auxiliary system of a heavy commercial vehicle. *Mech. Syst. Signal Process.* **2018**, *101*, 97–120. [CrossRef]

25.　Wu, B.; Lin, C.; Filipi, Z.; Peng, H.; Assanis, D. Optimization of power management strategies for a hydraulic hybrid Medium Truck. In Proceedings of the 2002 Advanced Vehicle Control Conference, Hiroshima, Japan, 9–13 September 2002.

26.　Jiao, X.; Shen, T. SDP Policy iteration-based energy management strategy using traffic information for commuter hybrid electric vehicles. *Energies* **2014**, *7*, 4648–4675. [CrossRef]